

Dynamical Critical Phenomena in three-dimensional Heisenberg Spin Glasses

Mitsuhiro Matsumoto, Koji Hukushima,* and Hajime Takayama

*Institute for Solid State Physics, University of Tokyo,
5-1-5 Kashiwa-no-ha, Kashiwa, Chiba 277-8581, Japan*

(Dated: November 20, 2018)

Spin-glass (SG) and chiral-glass (CG) orderings in three dimensional (3D) Heisenberg spin glass with and without magnetic anisotropy are studied by using large-scale off-equilibrium Monte Carlo simulations. A characteristic time of relaxation, which diverges at a transition temperature in the thermodynamic limit, is obtained as a function of the temperature and the system size. Based on the finite-size scaling analysis for the relaxation time, it is found that in the isotropic Heisenberg spin glass, the CG phase transition occurs at a finite temperature, while the SG transition occurs at a lower temperature, which is compatible with zero. Our results of the anisotropic case support the chirality scenario for the phase transitions in the 3D Heisenberg spin glasses.

I. INTRODUCTION

Chirality in frustrated magnets, which provides fascinating magnetic orderings and/or novel critical phenomena, has attracted interest in recent years¹. In the spin-glass (SG) study, the chirality-driven mechanism has been proposed by Kawamura² in order to explain the origin of experimentally observed SG phase transitions. The chirality scenario assumes that a chiral-glass (CG) long-range order exists at low temperatures with preserving the proper rotational symmetry in a fully isotropic SG model. By random magnetic anisotropy even of a small magnitude, which always exists in real experimental situations, a SG phase is expected to emerge as a result that the anisotropy mixes the two degrees of freedom, spin and chirality. Therefore, in the chirality-driven mechanism the SG phase transition experimentally observed in a class of compounds such as CuMn is essentially governed by the CG fixed point.

Some numerical results on equilibrium properties support that the chirality-driven phase transitions occur in a three dimensional (3D) Edwards-Anderson (EA) Heisenberg SG model^{3,4,5} as well as in a 3D XY SG model⁶. The CG transition temperature and the critical exponents are estimated. They seem to be compatible with those observed experimentally⁷. However, some researchers have argued the possibility of a finite-temperature SG transition⁸, or even simultaneous SG and CG transition in the 3D Heisenberg SG model⁹. In a 3D XY SG model, large scale domain-wall renormalization group calculation at zero temperature suggests that a SG long-range order occurs at non-zero temperature below the CG transition temperature¹⁰. A similar study obtained by different boundary conditions also support the existence of SG order at finite temperatures¹¹.

The observed critical behavior associated with the CG transition is found to be remarkably different from that observed in ordinary second-order phase transitions. For instance, the crossing of the Binder parameter of systems with different sizes at the transition temperature, which is usually observed in standard second-order transitions, never occurs in this model^{4,5}. Furthermore, the previous study revealed that the CG phase of the 3D

isotropic Heisenberg EA model had a peculiar feature which was consistent with one-step replica symmetry breaking (RSB) phase⁴. Some mean-field SG models with the one-step RSB exhibit dynamical singularity at a temperature well above the static transition temperature¹². Recent simulation on a mean-field SG model¹³ shows that dynamical finite-size scaling holds for the dynamical transition temperature which is different from the static one. It is of particular interest to clarify whether the CG phase of the 3D Heisenberg EA model belongs to this class or not.

Until now, there have been a few works on dynamical properties of the Heisenberg SG models. Olive et al¹⁴ and Yoshino and one of the authors (HT)¹⁵ investigated spin autocorrelation functions in *equilibrium* by Monte Carlo simulations. They found that, with the help of dynamical scaling analysis, the temperature dependence of the characteristic relaxation time is compatible with a zero-temperature SG transition. However, the corresponding CG relaxation time has not been investigated yet.

In the present paper, we study dynamical properties associated both with spin and chiral degrees of freedom above the transition temperature of the 3D Heisenberg EA model with and without anisotropic interactions. We developed an efficient method for extracting the equilibrium relaxation time from non-equilibrium simulation for a given finite-size system and analyzed the time scale by using the finite-size scaling. The results of our analyses on the isotropic Heisenberg SG model support the first assumption of the chirality mechanism, namely the existence of a finite temperature CG phase transition without a conventional SG long-range order. In particular, a crossover from high-temperature SG dominant regime to the CG dominant regime is clearly observed with decreasing temperature. In addition, by introducing a finite random anisotropic interaction, the SG relaxation time is found to be significantly enhanced at low temperatures and in systems with large sizes, while there is no such drastic change in the CG dynamics. This is consistent with the chirality mechanism.

Our work is distinct from the previous works in the following senses; (i) The CG dynamics as well as the

SG ones have been studied systematically both above and around a transition temperature, (ii) The equilibrium relaxation is estimated from non-equilibrium MC simulations. These results may be complementary with the previous equilibrium studies^{2,4}.

The present paper is organized as follows. In section II, we explain the model and the method of our Monte Carlo simulation. We introduce a dynamical ratio function and discuss its characteristic features in section III. Finite-size scaling of the characteristic time is studied in section IV and section V is devoted to summary of the paper.

II. MODEL AND SIMULATIONS

The model studied is a classical Heisenberg model on a simple cubic lattice, defined by the Hamiltonian,

$$H(\vec{S}) = - \sum_{\langle ij \rangle} J_{ij} \vec{S}_i \cdot \vec{S}_j - \sum_{\langle ij \rangle, \mu, \nu} D_{ij}^{\mu\nu} S_i^\mu S_j^\nu, \quad (1)$$

where $\vec{S}_i = (S_i^x, S_i^y, S_i^z)$ is a three-component unit vector, and the sum runs over all nearest-neighbor pairs with the total number of sites $N = L \times L \times L$. The nearest neighbor couplings J_{ij} are random bimodal variables which take $\pm J$ with equal probability. The anisotropic interactions $D_{ij}^{\mu\nu}$ are also independent random variables obeying a box distribution with its range $[-D : D]$. We assume that the anisotropic term is symmetric, $D_{ij}^{\mu\nu} = D_{ji}^{\nu\mu}$. A quite similar model has been studied by MC simulation¹⁶ with some values of strength D , where the SG phase at low temperatures has been found around and above $D/J \sim 0.05$. We study the model system both with the isotropic case ($D/J = 0$) and an anisotropic case ($D/J = 0.05$).

We employ a standard heat-bath Monte Carlo method with two sub-lattice flips¹⁴. One Monte Carlo step (MCS) is defined as N spin trials. We perform MC procedure as follows; firstly spins are set as a random configuration, namely they are instantaneously quenched from the high temperature limit. The spin configuration is updated at a working temperature T during a waiting time t_w , which is from 10^0 to 10^5 . Subsequently, additional MC steps are performed for measurements. The lattice sizes L studied are 4, 8, 16 and 32. In our simulations, we perform eight independent runs for each identical sample to take an average over initial conditions and different thermal noises. A typical number of samples averaged over is 40–960 depending on the system size.

In order to study non-equilibrium dynamics of the model, we calculate the spin autocorrelation function defined by

$$C_q(t_w, t) = \frac{1}{N} \sum_i [\langle \vec{S}_i(t_w) \cdot \vec{S}_i(t_w + t) \rangle], \quad (2)$$

where $\langle \dots \rangle$ represents an average over initial conditions and $[\dots]$ over the bond disorder. In the long time limit

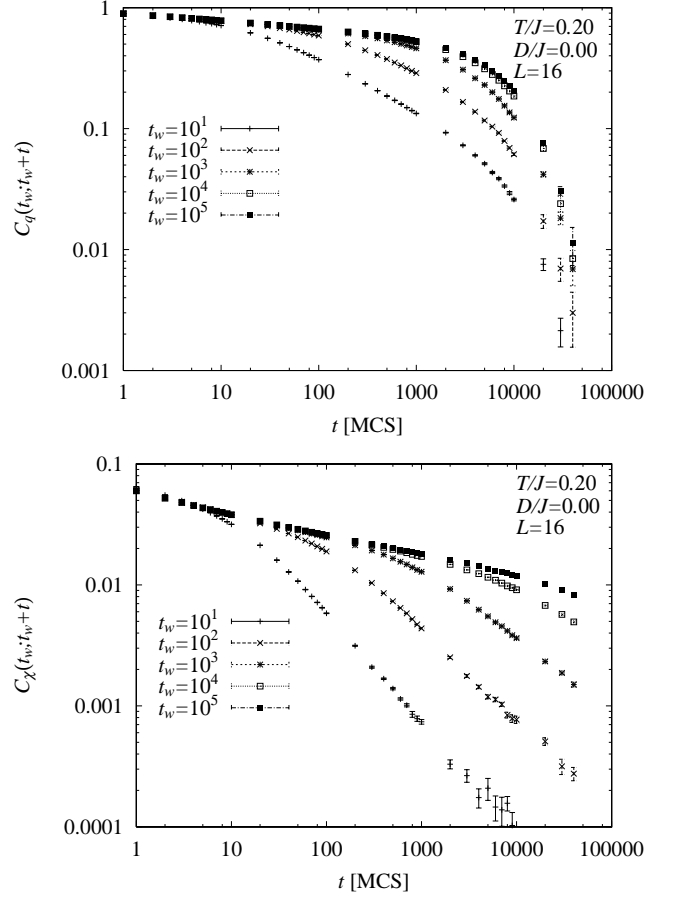


FIG. 1: Time dependence of the spin-glass (upper) and chiral-glass (lower) autocorrelation functions with different waiting times in the 3D isotropic Heisenberg SG model at $T/J = 0.20$. The system size is fixed, $L = 16$.

($t \rightarrow \infty$) after taking the equilibrium limit ($t_w \rightarrow \infty$) the autocorrelation, Eq. (2), converges to the SG order parameter originally proposed by Edwards and Anderson¹⁷. We also calculate the corresponding chirality autocorrelation function, which allows us to detect a possible CG transition from the dynamical point of view. It is also defined as an overlap of the local chirality

$$C_\chi(t_w, t) = \frac{1}{3N} \sum_i [\langle \vec{\chi}_i(t_w) \cdot \vec{\chi}_i(t_w + t) \rangle], \quad (3)$$

where $\chi_{i\mu}$ is the local chirality at the i th site and in the μ th direction defined by a scalar as

$$\chi_{i\mu} = \vec{S}_{i+\hat{e}_\mu} \cdot (\vec{S}_i \times \vec{S}_{i-\hat{e}_\mu}), \quad (4)$$

with \hat{e}_μ ($\mu = x, y, z$) being a unit lattice vector along the μ axis. The CG autocorrelation function in off-equilibrium has not been investigated extensively yet, except for Ref. 3.

In Fig. 1, we show the SG and CG autocorrelation functions with the different waiting times t_w against time t . In non-equilibrium dynamics, temporal correlation

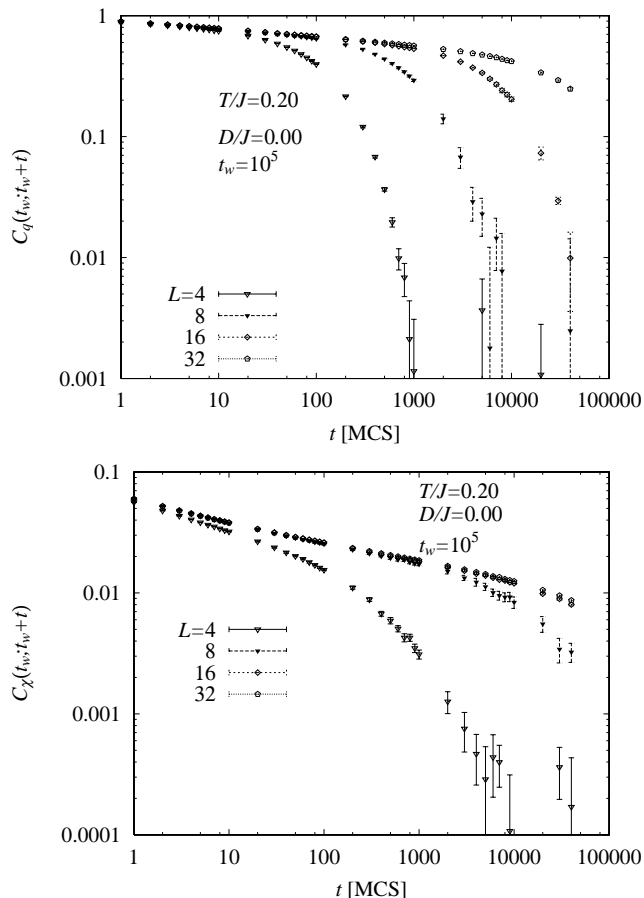


FIG. 2: Time dependence of the spin glass (upper) and chiral-glass (lower) autocorrelation functions with different sizes and the fixed waiting time $t_w = 10^5$ in the 3D isotropic Heisenberg SG model at $T/J = 0.20$.

functions explicitly depend on not only t but also t_w , which we call the breaking of time translational invariance. The longer is the waiting time, the slower becomes the relaxation. The curves with shorter waiting times start to deviate from an equilibrium function at the shorter time scales. Such a time scale, below which the time translational invariance holds effectively, is roughly proportional to the waiting time t_w .

In Fig. 2 we present the correlation functions with different system sizes for a fixed waiting time $t_w = 10^5$. One can clearly see that the relaxation curves start to deviate from that of the thermodynamic limit. This implies that finite-size effects yield another characteristic relaxation time. The latter is related to the critical slowing down which we study in the present work.

Generally speaking, equilibrium MC simulations for SG models suffer from extremely slow dynamics and equilibration is hardly realized in large systems at low temperatures. One of the advantages of the non-equilibrium simulation is to practically avoid such a very slow equilibration process. In the present work, we focus our attention to the longest relaxation time of finite-size sys-

tems which is expected to diverge with the system size at and below the transition temperature. Our strategy of the non-equilibrium simulation is to take the equilibrium limit, i.e., $t_w \rightarrow \infty$, after extracting the characteristic relaxation time under off-equilibrium in finite systems and then take the thermodynamic limit $L \rightarrow \infty$.

III. DYNAMICAL RATIO FUNCTION AND RELAXATION TIME

According to the dynamic scaling ansatz¹⁸, the autocorrelation function in equilibrium near a second-order phase transition has the form

$$C(t_w = \infty, t_w + t) \sim t^{-\lambda} f(t/\tau), \quad (5)$$

where τ is the relaxation time at a given temperature and λ a critical exponent. This form represents a crossover around τ from the short-time critical behavior, $t^{-\lambda}$, to the long-time relaxation described by $f(t/\tau)$. When the temperature approaches to the critical point T_c , the relaxation time τ diverges as $\tau(T) \sim |T - T_c|^{-z\nu}$. Thus, the autocorrelation function follows a power law in t at T_c .

One may consider that the critical temperature as well as the critical exponents associated with the transition can be easily obtained by the relaxation time near the critical temperature. There are, however, several difficulties in obtaining the relaxation time by MC simulations. One difficulty is due to extremely slow dynamics of SG systems as mentioned above. Another difficulty is that the method of obtaining the relaxation time requires accurate estimation of a long-time tail of the autocorrelation function. One way is to integrate $C(t)$ over time. A contribution to the integrated relaxation time is dominated by the long-time tail where $C(t)$ simulated is very small and largely fluctuating. Another method would be a fitting of $C(t)$ to a relaxation function with the scaled argument t/τ . It is, however, difficult to know the functional form explicitly, which is often non-exponential as seen in Fig. 1.

In order to avoid the above mentioned difficulties, Bhatt and Young¹⁹ (hereafter referred to as BY) have introduced a dimensionless dynamic correlation function

$$R_q(t_w, t_w + t) = \frac{C_q(t_w, t_w + t)}{\sqrt{\left\langle \left(\frac{1}{N} \sum_i \vec{S}_i(t_w) \cdot \vec{S}_i(t_w + t) \right)^2 \right\rangle}}. \quad (6)$$

The prefactor in Eq. (5) involving a power of t is canceled out by taking the ratio of moments. A similar dimensionless dynamical function has also been studied in simple ferromagnets^{20,21}. The corresponding CG ratio function

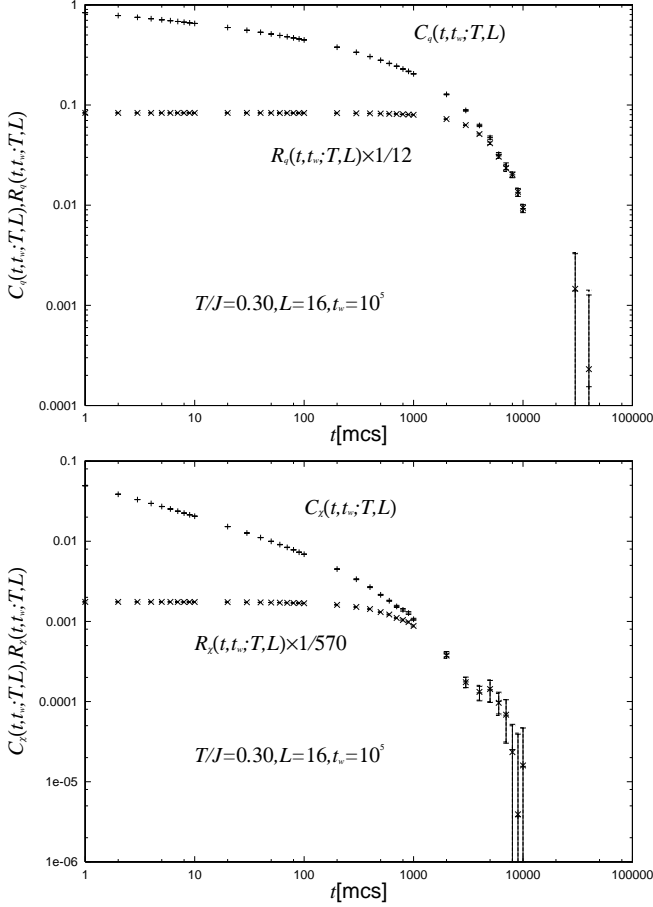


FIG. 3: Double logarithmic plot of the spin-glass (upper) and chiral-glass (lower) autocorrelation functions and ratio functions of the isotropic 3D Heisenberg spin glass model at $T/J = 0.30$.

is defined as

$$R_\chi(t_w, t_w + t) = \frac{C_\chi(t_w, t_w + t)}{\sqrt{\left\langle \left(\frac{1}{N} \sum_i \vec{\chi}_i(t_w) \cdot \vec{\chi}_i(t_w + t) \right)^2 \right\rangle}}. \quad (7)$$

Because these ratio functions are dimensionless such as the Binder parameter in the static case, the dynamical scaling form is expected to be given by a function of t/τ as

$$R(t) \sim \overline{R}(t/\tau), \quad (8)$$

where $\overline{R}(x)$ is a universal scaling function. BY¹⁹ fixed the waiting time t_w in Eq. (6) to t because it was believed that equilibration of the autocorrelation function on a given time scale t needed the waiting time t_w of the same time scale as t . They studied the dimensionless function of the short range Ising SG and the mean-field Sherrington-Kirkpatrick models just at the known critical temperature and successfully obtained the dynamical critical exponent z using the finite-size scaling for the relaxation times $\tau(L, T_c) \sim L^z$.

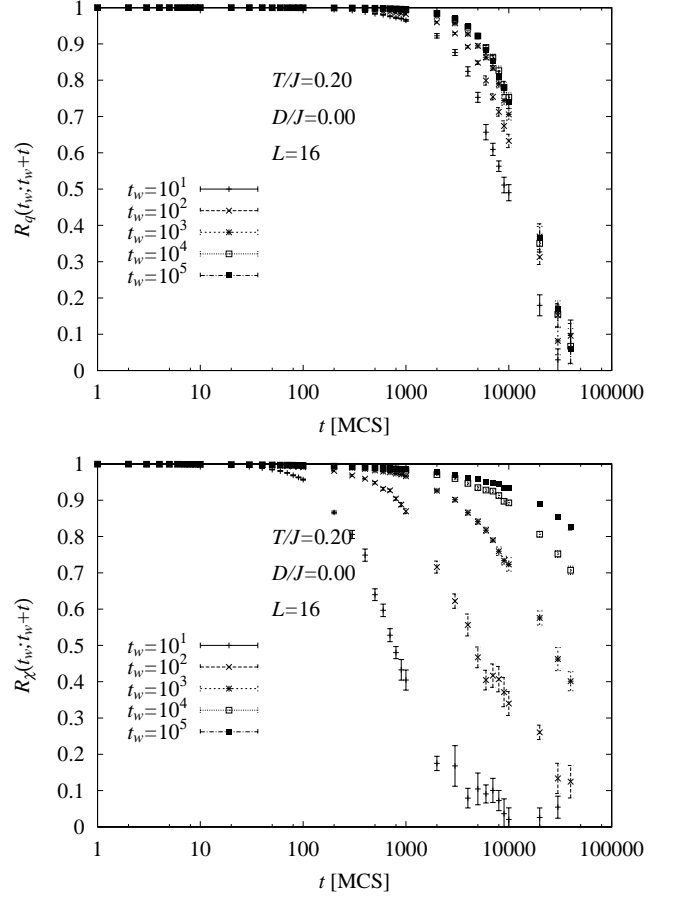


FIG. 4: Time dependence of the SG (upper) and CG (lower) ratio functions with different waiting times in the 3D isotropic Heisenberg SG model at $T/J = 0.20$.

In the present study, we systematically investigate the ratio function both for the SG and CG autocorrelation functions as bivariate functions of t and t_w . Instead of taking the equilibrium limit of the ratio function or fixing the time scale $t_w \sim t$ studied previously, we try to take the equilibrium limit ($t_w \rightarrow \infty$) of the relaxation time $\tau(t, t_w)$ obtained from the ratio function for several waiting times.

Equations (6) and (7) are the ratio of an odd moment of the autocorrelation function to an even one. Consequently, the ratio functions for a given t_w decay from 1 at $t = 0$ to zero as t goes to infinity and they are sensitive to flips or rotations of the entire system, which are the longest mode of relaxation. Therefore we expect that the ratio functions pick up only slowest relaxation modes from the whole modes of $C(t)$. A typical example of the ratio function, as well as $C(t)$, is presented for the SG and CG autocorrelations in Fig. 3. As expected, the ratio functions are unity in the relatively short-time regime, implying that the denominator and the numerator coincide with each other. For the longer-time regime, as shown in the figure, the ratio functions of spin and chirality sector coincide with the tail of the corresponding

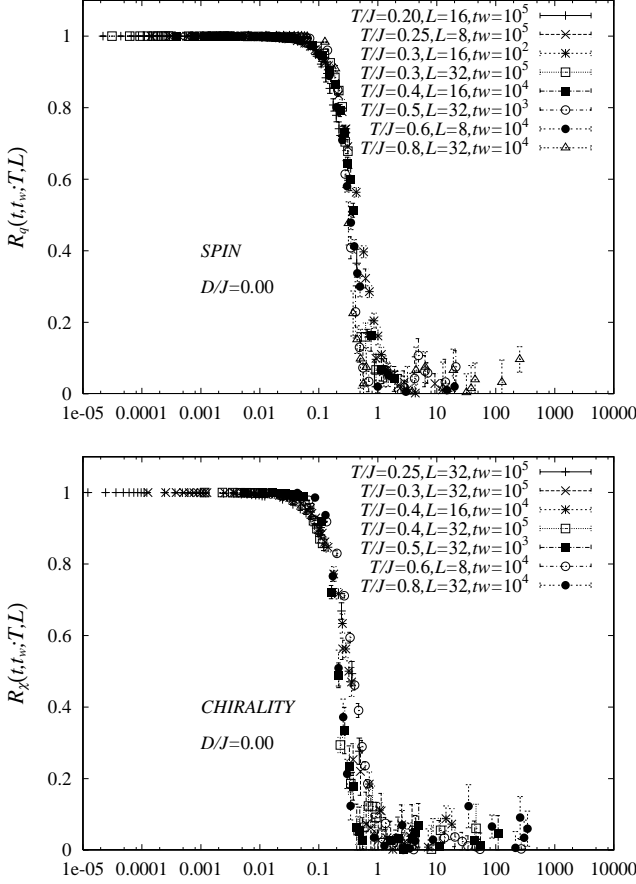


FIG. 5: Scaling plot of the SG(upper) and CG(lower) ratio functions of the 3D Heisenberg SG model with various temperatures, waiting times and system sizes.

autocorrelation function multiplied by a certain constant, which represents a statistical weight of the slowest modes in $C(t)$.

When the ratio function $R(t)$ extracts only one relaxation mode corresponding to the longest mode in the system, it is expected to show a universal scaling form and to be scaled as

$$R(t_w, t_w + t; T, L) \sim R(t/\tau(t_w; T, L)). \quad (9)$$

Here we assume that the ratio functions depend on t_w , T and L only through the relaxation time. This may be an extension of the dynamical scaling (8) to an off-equilibrium situation, which is to be checked. We try to scale the observed ratio functions into a universal scaling function by appropriately choosing the time constant τ depending on t_w , T and L . Figure 5 presents a result of the scaled ratio functions for $D/J = 0$. In the figure, one sees that both the SG and CG ratio functions with various temperatures, system sizes and waiting times are almost scaled as a common universal function. Note that this finding allows us to compare the absolute values of the SG and CG relaxation time. Using the scaling of the ratio functions in this way, we obtain the characteristic

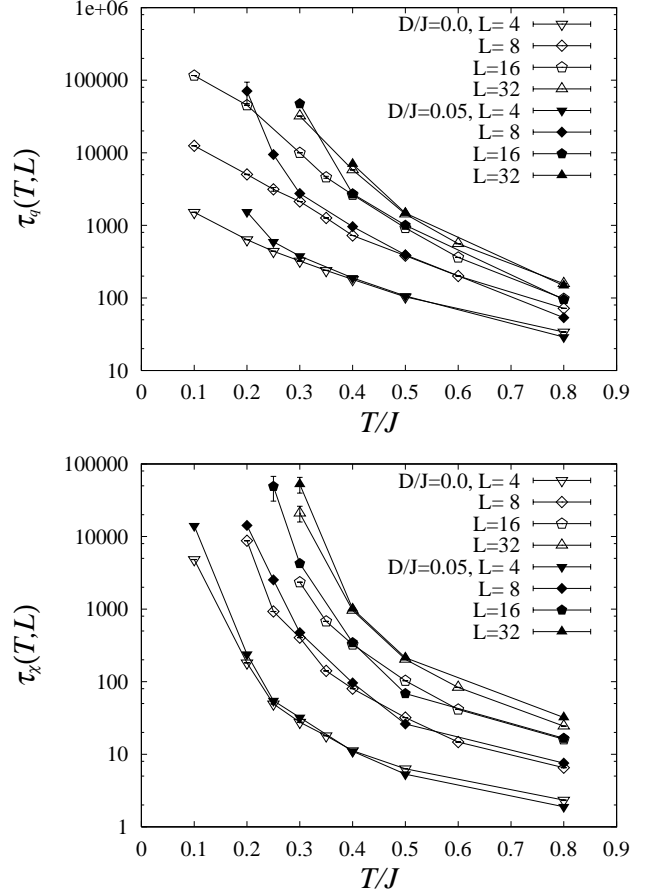


FIG. 6: Temperature dependence of the SG (upper) and CG (lower) relaxation times in equilibrium for the isotropic case (open marks) and anisotropic case with $D/J = 0.05$ (filled marks).

relaxation times $\tau(t_w; T, L)$ for each set of parameters t_w , T and L . We then let t_w to go to infinity to obtain the characteristic relaxation times in *equilibrium*. We assume that the t_w -dependence of the relaxation times is described as

$$\tau(t_w; T, L) = \tau(t_w = \infty; T, L) - \alpha t_w^{-\beta}, \quad (10)$$

with α, β being some constants and $\tau(T, L) \equiv \tau(t_w = \infty; T, L)$ the equilibrium relaxation time.

Temperature dependences of $\tau(T, L)$ thus extracted are shown in Fig. 6 for the spin (upper) and chiral (lower) degrees of freedom. We first note that the CG relaxation time is almost independent of the strength of the magnetic anisotropy D . This is natural since the anisotropy breaks the rotational symmetry, but not the reflection symmetry which is spontaneously broken by the CG phase transition. On the other hand, as seen in Fig. 6, the random anisotropy changes drastically the behavior of the SG relaxation time. The SG relaxation time of $D/J = 0.05$ increases rapidly around $T/J = 0.25$ with decreasing the temperature. Such a drastic change of the behavior implies that the anisotropy mixes the chirality

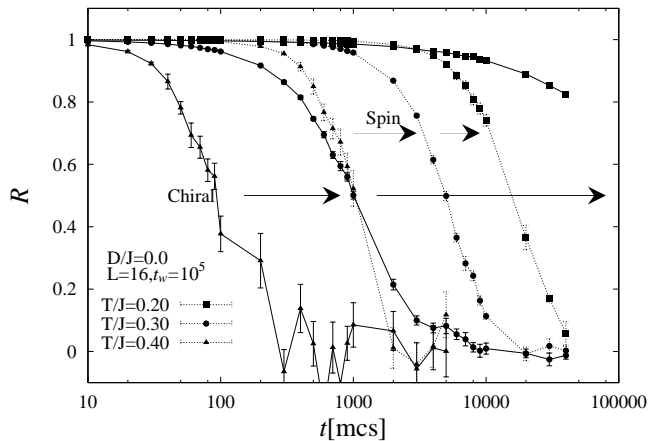


FIG. 7: Time evolution of the SG (solid) and CG (dotted) ratio functions at $T/J = 0.40, 0.30$ and 0.20 from left to right.

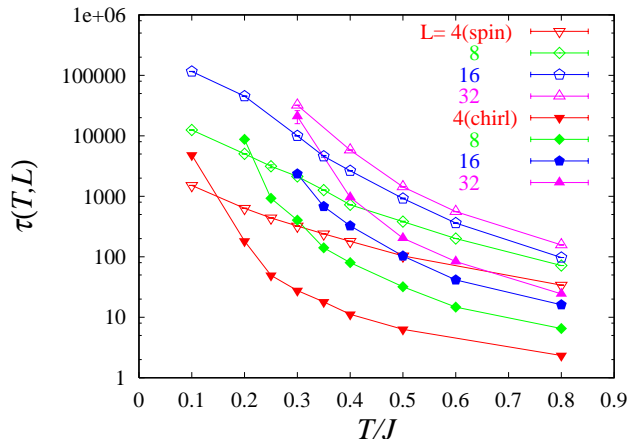


FIG. 8: Temperature dependence of the SG (open) and CG (filled) relaxation times in equilibrium in the isotropic case with different sizes.

with spin degrees of freedom as predicted in the chirality scenario. This is the first observation of the effect of the anisotropy for the SG relaxation times.

We can show another evidence that the chirality dominates the phase transition in the isotropic 3D Heisenberg SG model. In Fig. 7, the time evolution of SG (broken line) and CG (solid line) ratio functions at $T/J = 0.40, 0.30$ and 0.20 with $L = 16$ and $t_w = 10^5$ are shown simultaneously. The characteristic relaxation time of the CG ratio function becomes larger with decreasing temperature much more rapidly than that of the SG ratio function does and it finally exceeds the SG relaxation time at $T/J = 0.20$. This fact strongly suggests that the CG degrees of freedom dominate large-scale and long-time phenomena at low temperatures, while the SG one dominates at relatively high temperatures. This type of crossover is observed at the first time in the present work. We can also see such a crossover in the resulting

equilibrium relaxation time. Figure 8 shows the same data as shown in Fig. 6 but only for the isotropic case $D/J = 0$. A characteristic temperature at which the two relaxation times cross each other shifts towards the high-temperature side as the system size increases. We emphasize that this crossover is not due to an apparent finite-size effect.

IV. FINITE-SIZE SCALING

In the present section we discuss the finite-size-scaling analysis of the equilibrium relaxation time obtained in the previous section. According to a standard dynamical finite-size-scaling analysis, the scaling form of $\tau(T, L)$ is given by

$$\tau(T, L) \sim L^z \bar{\tau} \left((T - T_c) L^{1/\nu} \right), \quad (11)$$

where z is the dynamical critical exponent and ν the correlation-length exponent. The scaling function becomes a constant just at the critical temperature, leading the finite-size scaling form, $\tau(T_c, L) \sim L^z$, previously studied¹⁹. We discuss asymptotic behavior of the scaling function $\bar{\tau}(x)$. In a large-system-size limit above T_c , i.e., $x \gg 1$, the scaling of Eq. (11) should recover an ordinary scaling form,

$$\tau(T, L = \infty) \sim (T - T_c)^{-z\nu}. \quad (12)$$

This leads that the scaling function behaves as

$$\bar{\tau}(x) \sim x^{-z\nu} \quad (13)$$

at $x \gg 1$. Assuming that the transition takes place at a finite temperature, the opposite limit, i.e. $-x \gg 1$, can be also argued in the isotropic case where the system would entirely behave like a rigid magnet. For the SG ordering in $D/J = 0$, such a system rotates globally as coherent diffusive motion with the relaxation time τ_D proportional to the bulk volume. This implies that the asymptotic scaling form of the SG relaxation time in $D/J = 0$ is

$$\bar{\tau}(x) \sim |x|^{(d-z)\nu}, \quad (14)$$

in the limit $-x \gg 1$ with d being the dimensionality. The asymptotic scaling function for the CG relaxation time, however, would follow an exponential activated type because of the discrete nature of chirality.

The situation is complicated in a system with $T_c = 0$. In one case where the conventional form (11) holds with $T_c = 0$ as in the standard second-order phase transition, the scaling function in the asymptotic limit at $x \ll 1$, $\bar{\tau}(x = 0)$, becomes a constant. On the other hand, Yoshino and Takayama¹⁵ proposed a modified scaling form which was a combination of the standard form (11) with $T_c = 0$ and the diffusion relaxation time, $\tau_D \sim L^d/T$. This form is compatible with (11) and (14) in the limit $x \ll 1$ if $(d - z)\nu = -1$ holds. In this case, the scaling exponents, z and ν , are no longer independent parameters.

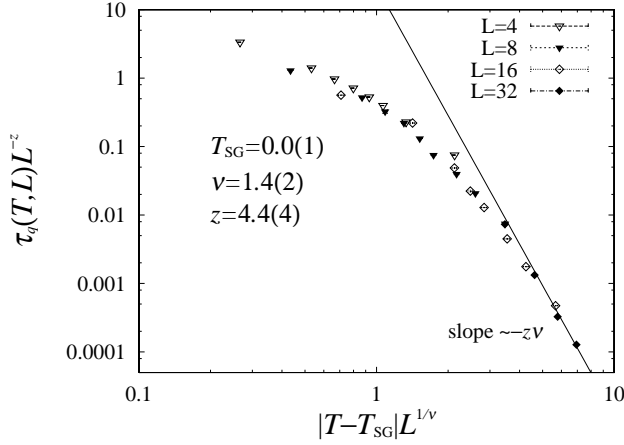


FIG. 9: Finite-size scaling plot of the SG relaxation time in the isotropic 3D Heisenberg SG model. The parameters of the scaling are as follows : $T_{SG} = 0.0(1)$, $\nu = 1.4(2)$ and $z = 4.4(4)$. The solid line represents the expected asymptotic behavior for large scaling regime.

A. Isotropic case: $D/J = 0$

The result of the finite-size scaling analysis mentioned above is demonstrated for the SG relaxation times of the isotropic Heisenberg SG model in Fig. 9. As can be seen from the figure, the data points are found to collapse into the universal scaling function. From the scaling we estimate $T_{SG} = 0.0(1)$, $\nu = 1.4(2)$ and $z = 4.4(4)$. Our result for the SG transition temperature is roughly consistent with the zero-temperature phase transition^{14,15,16,22,23}, although we could not completely exclude the possibility of the SG phase transition at a very low but finite temperature. Assuming the zero-temperature transition, the scaling results suggest that relaxation times diverge with a power law of T as T goes to 0, but not an exponential divergence which occurs at the lower critical dimensions such as the two-dimensional Ising SG model.

We expect that the scaling function converges to a finite value in the limit $x \rightarrow 0$ as in the standard second-order phase transition, though we don't have enough data to confirm this convergence. The scaling plot may be consistent with a modified scaling from $x \gg 1$ to $x \ll 1$ proposed by Yoshino and Takayama¹⁵, but then temperature dependence of the relaxation time at low temperatures, $\tau \sim T^{(d-z)\nu}$ with z and ν obtained above does not coincide with that expected from a simple diffusive relaxation time proportional to $1/T$. A further investigation is needed to clarify this point.

The present estimate for ν is compatible with the previous ones in other works; $\nu = 1.54(19)$ ²³ and $2.0(2)$ ² by a domain-wall renormalization group calculation at $T = 0$, $\nu = 1.35(5)$ by a MC simulation¹⁶, $\nu \sim 1.6$ by an equilibrium dynamics¹⁵ and $\nu \sim 1.14$ by a MC simulation¹⁴.

We have also analyzed the CG relaxation time by a similar scaling. The best scaling shown in Fig. 10 is

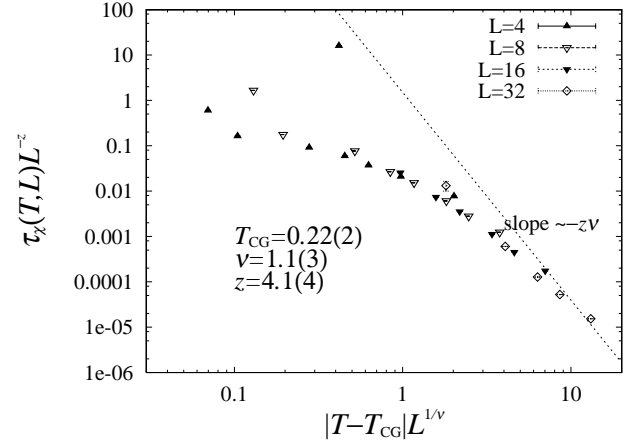


FIG. 10: Finite-size scaling plot of the CG relaxation time in the isotropic 3D Heisenberg SG model. The parameters of the scaling are as follows; $T_{CG} = 0.22(2)$, $\nu = 1.1(3)$ and $z = 4.1(4)$.

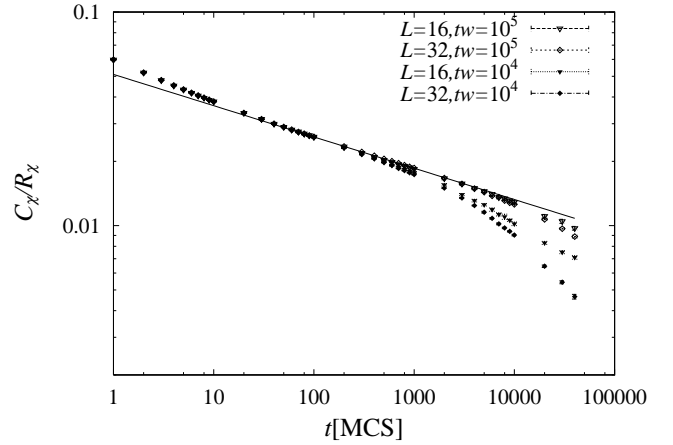


FIG. 11: Time dependence of C_χ/R_χ for the CG at $T/J = 0.20$.

obtained by the following estimates: $T_{CG} = 0.22(2)$, $\nu = 1.1(3)$ and $z = 4.1(4)$. The estimate for T_{CG} is consistent with the recent equilibrium MC calculations^{24,25}. The present estimate for ν is rather close to the previous MC estimate for the Gaussian distribution, $\nu \sim 1.2$ ⁴.

At the critical temperature, the autocorrelation function C_χ and also C_χ/R_χ follow the algebraic decay (5) with the exponent $\lambda = \beta/z\nu$. In Fig. 11 we show C_χ/R_χ as a function of time at $T/J = 0.20$ close to the CG transition temperature. The data still depend on both the system size and the waiting time. As a preliminary study, we estimate the exponent $\lambda = 0.23(5)$ from the slope of the plot, where the numerical error comes from the uncertainty of the critical temperature. This value combined with z and ν by the finite-size scaling leads to another exponent, $\beta \sim 1.0$, which is consistent with the previous work³.

As mentioned in the introduction, the dynamical phase

transition which is separated from the static one can exhibit at a finite temperature in some one-step RSB systems. It depends on whether the order parameter continuously appears or discontinuously jumps up at the static transition as the temperature decreases. Examples of the discontinuous one-step RSB transition are the mean-field p -spin glass with $p > 2$ and the mean-field q -state Potts glass with $q > 4$, while those of the continuous one-step RSB transition are the mean-field q -state Potts glass with $2.8 < q \leq 4$. Our estimation of the CG transition temperature by the dynamical finite-size scaling is consistent with the static transition temperature. This fact means that the CG phase belongs to the latter class of the one-step RSB.

B. Anisotropic case : $D/J = 0.05$

The finite-size scaling plots of the CG relaxation times in the anisotropic 3D Heisenberg SG model is shown in Fig. 12. In the analysis we regard the CG critical temperature as a unique adjustable parameter, and obtain $T_{CG} = 0.24(2)$. As seen in Fig. 12, the scaling analysis works well for both $D/J = 0.0$ and 0.05 with the common z and ν . This implies that the critical exponents associated with the CG critical phenomena as well as the scaling function are independent of the anisotropic term. This finding of our analysis is consistent with the expectation that the anisotropic interactions are expected not to affect the CG symmetry.

We believe that the SG phase transition also occurs in the anisotropic case at the same temperature as the CG transition temperature. In fact, we have found in Fig. 6 that the anisotropic term significantly enhances the SG relaxation time at low temperatures. Unfortunately, however, such enhanced relaxation time appears only in larger sizes and at lower temperatures. Therefore, these data points are not enough to test the finite-size scaling.

V. DISCUSSIONS

We have studied dynamical critical phenomena in the 3D Heisenberg SG models using Monte Carlo simulations. Our results support the chirality scenario for realistic SG transitions. It is confirmed that in the fully isotropic model at low temperatures, the CG relaxation time exceeds the SG relaxation time. This result strongly suggests that long-time or large scale behavior is dominated by the CG ordering. The finite-size-scaling analysis of the relaxation time supports that the CG phase transition with the diverging relaxation time occurs at a finite temperature, while the SG phase transition takes place at a lower temperature, consistent with even at zero temperature as previously studied^{14,15,16,22,23}. In other words, the spontaneous breaking of discrete Z_2 symmetry likely occurs with preserving the proper rotational symmetry $SO(3)$. The SG and CG transition tempera-

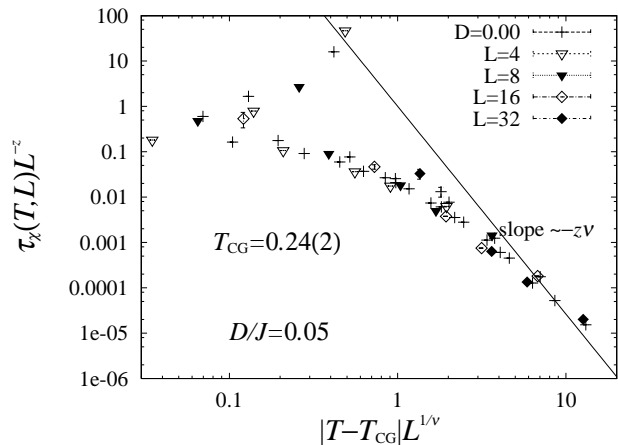


FIG. 12: Finite-size scaling plot of the CG relaxation time in the 3D Heisenberg SG model with $D/J = 0.05$. The parameter of the scaling is the CG transition temperature $T_{CG} = 0.24(2)$. The scaling data of $D/J = 0$ shown in Fig. 10 are also plotted with the cross mark.

tures of our result are significantly separated with each other within numerical accuracy. This is the first support for the basic assumption of the chirality scenario from a dynamical point of view.

We have also studied an anisotropic 3D Heisenberg SG model in the similar way. It is found that by introducing the weak random anisotropy, the SG relaxation times in the large system sizes increase at low temperatures, similar to that observed in the CG relaxation time, although a finite-temperature SG phase transition cannot be directly determined by the finite-size-scaling analysis. Our finite-size-scaling analysis of the CG relaxation time strongly suggests, on the other hand, that the CG phase transition with the anisotropic interactions belongs to the same universality class as the isotropic case. When the SG phase transition in the anisotropic case is intrinsically dominated by the SG order parameter but not the CG order parameter, the observed CG critical behavior should be affected by the SG transition and it should be different from the fully isotropic case. Therefore, from this point of view, our result is consistent with the chirality mechanism where the phase transition is dominated by the CG order parameter. In order to further clarify the nature of phase transition in the anisotropic case, however, directly measurements of the SG phase transition and its critical exponents are required.

A standard scenario²⁶ based on the zero-temperature SG transition in the isotropic point says that the SG transition continuously approaches to zero in the zero anisotropy limit as $T_{SG}(D) \propto D^{1/4}$; see Fig. 13(a). Because the anisotropy reduces the symmetry of Hamiltonian, the universality class changes from the isotropic SG to the anisotropic SG. The latter is expected to be in the class of the Ising SG. On the other hand, according to the chirality mechanism², the random magnetic anisotropy D plays a role of mixing the CG long-range order with the

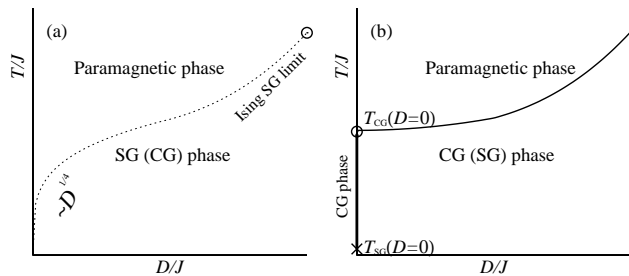


FIG. 13: A schematic picture of a phase diagram in the standard scenario (left) and the chirality scenario (right).

SG one. The SG transition temperature in the ideal zero anisotropy limit is predicted to coincide with $T_{CG}(D=0)$ but not $T_{SG}(D=0)$, as shown in Fig. 13(b). This may be true wherever $T_{CG} > T_{SG}$ at the isotropic limit even with $T_{SG}(D=0) > 0$. Once the CG has a long-range order, even the small anisotropy D coherently breaks the rotational symmetry of the system. Consequently, the SG critical behavior observed in the anisotropic model is governed by the fixed point of the CG transition of the isotropic model. The two scenarios can in principle be distinguished by the phase boundary near the isotropic

limit and the universality class along the phase boundary. Our findings that the CG universality class is not affected by the anisotropy D and that $T_{SG} < T_{CG}$ in the isotropic system prefer the chirality scenario.

In summary, spin-glass and chiral-glass orderings in three-dimensional Heisenberg spin glass model are studied from the point of view of dynamics by off-equilibrium Monte Carlo simulations. Our results support the chirality scenario for the SG phase transition in three dimensions.

Acknowledgements

The authors would like to thank H. Kawamura for useful discussions. This work is supported by a Grant-in-Aid for Scientific Research Program (# 12640367) and that for the Encouragement of Young Scientists(# 13740233) from the Ministry of Education, Science, Sports, Culture and Technology of Japan. The numerical calculations were mainly made by use of the Hitachi SR8000/60 at the Supercomputer Center, Institute for Solid State Physics, the University of Tokyo.

* Electronic address: hukusima@issp.u-tokyo.ac.jp

¹ H. Kawamura, J. Phys. Condens. Matt. **10**, 4707 (1998).

² H. Kawamura, Phys. Rev. Lett. **68**, 3785 (1992).

³ H. Kawamura, Phys. Rev. Lett. **80**, 5421 (1998).

⁴ K. Hukushima and H. Kawamura, Phys. Rev. E **61**, R1011 (2000).

⁵ H. Kawamura and D. Imagawa, Phys. Rev. Lett. **87**, 207203 (2001).

⁶ H. Kawamura and M. S. Li, Phys. Rev. Lett. **87**, 187204 (2001).

⁷ D. Petit, L. Fruchter, I. A. Campbell, Phys. Rev. Lett. **83**, 5130 (1999); D. Petit, L. Fruchter, I.A. Campbell, cond-mat/0111129

⁸ F. Matsubara, T. Shirakura and S. Endo, Phys. Rev. B **64**, 092412 (2001).

⁹ T. Nakamura and S. Endoh, cond-mat/0110017.

¹⁰ J. Maucourt and D. R. Grempel, Phys. Rev. Lett. **80**, 770 (1998).

¹¹ J. M. Kostelitz and N. Akino, Phys. Rev. Lett. **82**, 4094 (1999).

¹² For review on spin glasses; see K. H. Fischer and J. A. Hertz, *Spin Glasses* (Cambridge University Press, Cambridge, 1991); A. P. Young, *Spin Glasses and Random Fields* (World Scientific, Singapore, 1997).

¹³ C. Brangian, W. Kob and K. Binder, Europhys. Lett. **53**,

756 (2001).

¹⁴ J. A. Olive, A. P. Young and D. Sherrington, Phys. Rev. B **34**, 6341 (1986).

¹⁵ H. Yoshino and H. Takayama, Europhys. Lett. **22**, 631 (1993).

¹⁶ F. Matsubara, T. Iyoda and S. Inawashiro, Phys. Rev. Lett. **67**, 1458 (1991).

¹⁷ S. Edwards and P. W. Anderson, J. Phys. F **5**, 965 (1975).

¹⁸ P. C. Hohenberg and B. I. Halperin, Rev. Mod. Phys. **49**, 435 (1977).

¹⁹ R. N. Bhatt and A. P. Young, Europhys. Lett. **20**, 59 (1992).

²⁰ A. Jaster, J. Mainville, L. Schulke and B. Zheng, J. Phys. A **32**, 1395 (1999).

²¹ Y. Okabe, Y. Tomita and K. Kaneda, J. Phys. Soc. Jpn. **69** Suppl., 199 (200)

²² J. R. Banavar and M. Cieplak, Phys. Rev. Lett. **48**, 832 (1982).

²³ W. L. McMillan, Phys. Rev. B **31**, 342 (1985).

²⁴ D. Imagawa and H. Kawamura, J. Phys. Soc. Jpn. **71**, 127 (2002).

²⁵ K. Hukushima and H. Kawamura, private communication

²⁶ B. W. Morris, S. G. Colborne, M. A. Moore, A. J. Bray, and J. Canisius, J. Phys. C **19**, 1157 (1986).